

over time more visible. For this reason, sinc interpolation has been recommended for such applications [5]. The image space implementation of sinc interpolation can be very slow unless the interpolation kernel is severely truncated, which may result in ringing artifacts. Unser *et al.* [6], Fraser *et al.* [7], and Eddy *et al.* [8] each separately proposed a faster technique using three shearing transformations to perform a 2-D rotation, and implementing the interpolation within each sheared row/column using (1). The methods put forward in the present correspondence clarify the results of [4] and show how multidimensional Fourier transforms can be used to perform image rotations directly. These techniques can be combined with other Fourier space processing, if desired (e.g., sharpening, differentiation, etc.).

#### REFERENCES

- [1] L. R. Rabiner, R. W. Schafer, and C. M. Rader, "The chirp  $z$ -transform algorithm and its application," *Bell Syst. Tech. J.*, vol. 48, pp. 1249–1292, 1969.
- [2] D. H. Bailey and P. N. Swartztrauber, "The fractional Fourier transform and applications," *SIAM Rev.*, vol. 33, pp. 389–404, 1991.
- [3] S. Ljunggren, "A simple graphical representation of Fourier-based imaging methods," *J. Magn. Reson.*, vol. 54, pp. 338–343, 1983.
- [4] W. M. Lawton, "Multidimensional chirp algorithms for computing Fourier transforms," *IEEE Trans. Image Processing*, vol. 1, pp. 429–431, 1992.
- [5] J. V. Hajnal *et al.*, "A registration and interpolation procedure for subvoxel matching of serially acquired MR images," *J. Comput. Assist. Tomogr.*, vol. 19, pp. 289–296, 1995.
- [6] M. Unser, P. Thévenaz, and L. Yaroslavsky, "Convolution-based interpolation for fast, high-quality rotation of images," *IEEE Trans. Image Processing*, vol. 4, pp. 1371–1381, 1995.
- [7] D. Fraser and R. A. Schowengerdt, "Avoidance of additional aliasing in multipass image rotations," *IEEE Trans. Image Processing*, vol. 3, pp. 721–735, 1994.
- [8] W. F. Eddy, M. Fitzgerald, and D. C. Noll, "Improved image registration by using Fourier interpolation," *Magn. Reson. Med.*, vol. 36, pp. 923–931, 1996.

## $\mathcal{L}$ -M-S Filters for Image Restoration Applications

Doina Petrescu, Ioan Tăbuș, and Moncef Gabbouj

**Abstract**—A new filtering architecture is proposed, generalizing some previously introduced multilevel median filters. An efficient design procedure for the new filtering architecture is demonstrated for image restoration application. Simulation results show a good noise rejection performance, combined with a fine detail preservation capability.

**Index Terms**—Median filters, multistage filtering architecture, stack filters.

Manuscript received December 16, 1996; revised May 5, 1998. The associate editor coordinating the review of this manuscript and approving it for publication was Prof. Stephen E. Reichenbach.

D. Petrescu was with the Signal Processing Laboratory, Tampere University of Technology, SF-33101 Tampere, Finland. She is now with Nokia Research Center, FIN-33720 Tampere, Finland.

I. Tăbuș and M. Gabbouj are with the Signal Processing Laboratory, Tampere University of Technology, SF-33101 Tampere, Finland.

Publisher Item Identifier S 1057-7149(99)06816-5.

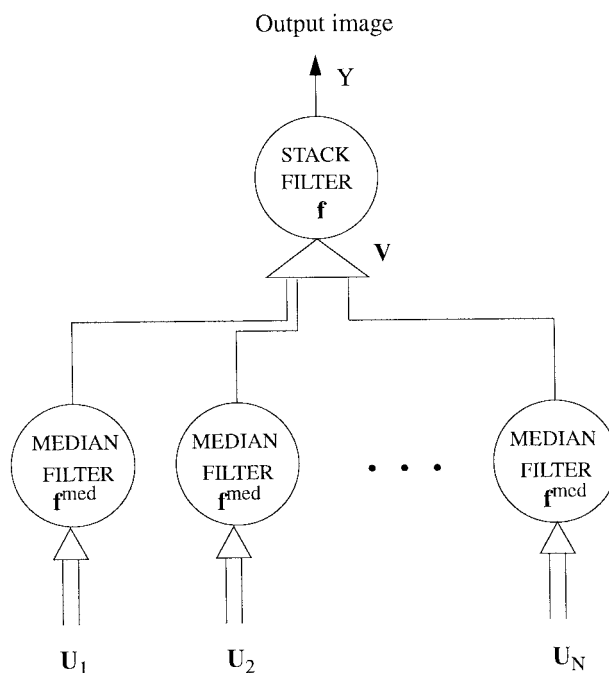


Fig. 1.  $\mathcal{L}$ -M-S filter architecture.

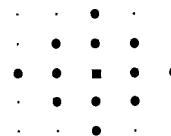


Fig. 2. Thirteen-pixel window shape.

## I. INTRODUCTION

Median filtering is efficiently used as an impulsive noise smoother for different signal and image processing applications. Although noise rejection is obtained, standard median filters have poor performance in preserving small details in images. The larger the filter window is, the better noise attenuation is obtained, but the worse detail preservation is achieved. Several solutions were proposed to improve the ability of median filtering to preserve particular features. One type of solutions replaced the standard median filter with weighted median or median-type filters optimally designed to preserve features of given shapes and sizes, [8]. Other types of solutions were introduced in [1], [4], as multilevel, nonadaptive, structure-preserving filtering architectures. These methods consist in combining in a median filtering stage the outputs of several subfilters (finite impulse response, median), spanning subwindows with different orientations inside the processing mask. Each subfilter is designed to preserve a feature in one fixed direction. Details covered by the subfilters are well restored, but thin lines along other directions are often distorted. Two-level architectures based on median or related filter classes have also been proposed in [6] and [9].

Almost all these filtering solutions have a positive Boolean function representation in the binary domain, and they belong to the larger class of stack filters [7]. Designing an optimal stack filter for a training

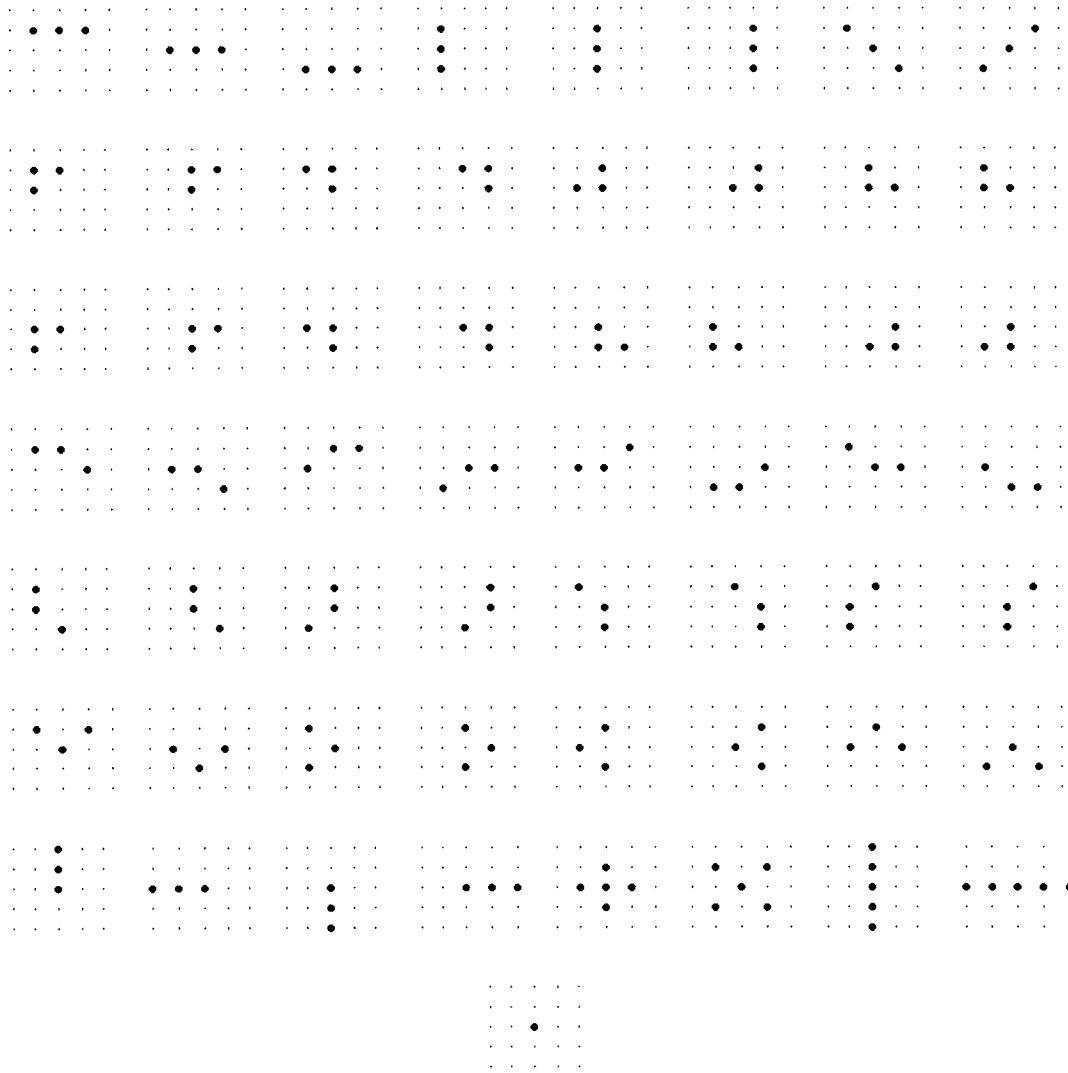


Fig. 3. Structural elements of the library.

set allows better noise attenuation as well as detail preservation [5]. However, the optimal stack filter design [2] problem has no tractable solution for very large processing masks since the computational complexity for the optimal stack filter design grows exponentially with the number of inputs in the processing mask.

In this work, a two-level filtering architecture is proposed for image restoration applications, aiming to achieve the impulsive noise rejection properties of median filters and the detail preservation ability of stack filters. The configurable subwindow structure used in the first level of the architecture allows more flexibility than multilevel median filters.

This correspondence is organized as follows: In Section II the new filtering architecture is introduced and the library–median–stack ( $\mathcal{L}$ –M–S) filter class is defined. The optimality inside ( $\mathcal{L}$ –M–S) filter class is discussed in Section III, where an efficient design procedure is proposed. An extensive experimental analysis for different images and different perturbation scenarios is presented in Section IV. Section V summarizes the main conclusions.

## II. ARCHITECTURE OF $\mathcal{L}$ –M–S FILTERS

The purpose of the  $\mathcal{L}$ –M–S filter class is to generalize previous multilevel median filtering architectures, combining the beneficial

properties of median filters for small processing masks with the fine tuning properties of stack filters for larger processing masks. To this end, a two-level filtering structure is proposed. In the first level,  $N$  median filters using different masks, selected from the library  $\mathcal{L}$ , are applied in parallel to the input image. In the second level, a stack filter processes the outputs of the first level median filters, yielding the overall output.

We denote the stack filtering performed in the integer domain by  $SF_{\mathbf{f}}$ , where  $\mathbf{f}$  is the positive Boolean function describing the filter in the thresholded binary domain.

Denote by  $\{\mathcal{L}, N\}$  the  $\mathcal{L}$ –M–S filter class (or structure), where  $N$  is the number of median filters in the first stage and  $\mathcal{L} = \{\mathcal{L}_1, \dots, \mathcal{L}_K\}$  is the library containing  $K$  subwindows of the large processing mask  $\mathbf{X}$ . A  $\mathcal{L}$ –M–S filter belonging to the filter class  $\{\mathcal{L}, N\}$  is specified by a positive Boolean function  $\mathbf{f}$  and some indices  $\ell_1, \dots, \ell_N$  and operates in the following way (see Fig. 1): the indices  $\ell_1, \dots, \ell_N$  select from the library the subwindows for the median filters in the first level  $\mathbf{U}_1 = \mathcal{L}_{\ell_1}, \dots, \mathbf{U}_N = \mathcal{L}_{\ell_N}$ . The outputs of the median filters are inputs to the stack filter  $SF_{\mathbf{f}}$ . The stack filter output is the output of the  $\mathcal{L}$ –M–S filter, as follows:

$$Y = SF_{\mathbf{f}}(\mathbf{V}) = SF_{\mathbf{f}}([\text{median}(\mathbf{U}_1) \cdots \text{median}(\mathbf{U}_N)]). \quad (1)$$

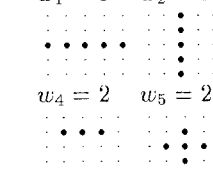
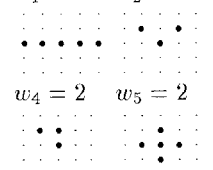
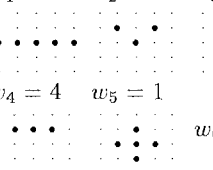
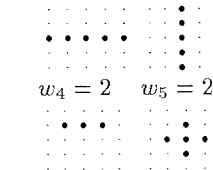
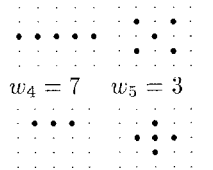
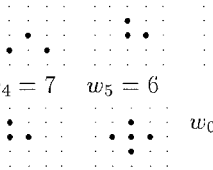
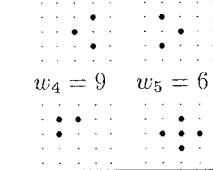
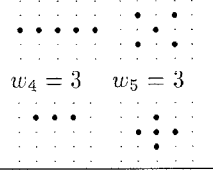
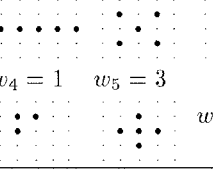
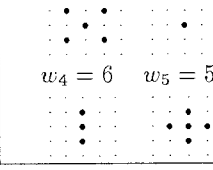
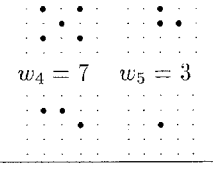
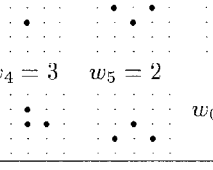
	Lena	Airfield	Bridge
SNR=3dB	$w_1 = 3$ $w_2 = 2$ $w_3 = 2$  $w_4 = 2$ $w_5 = 2$ $w_0 = 6$	$w_1 = 3$ $w_2 = 2$ $w_3 = 2$  $w_4 = 2$ $w_5 = 2$ $w_0 = 6$	$w_1 = 2$ $w_2 = 4$ $w_3 = 2$  $w_4 = 4$ $w_5 = 1$ $w_0 = 7$
SNR=6dB	$w_1 = 3$ $w_2 = 2$ $w_3 = 2$  $w_4 = 2$ $w_5 = 2$ $w_0 = 6$	$w_1 = 4$ $w_2 = 6$ $w_3 = 2$  $w_4 = 7$ $w_5 = 3$ $w_0 = 12$	$w_1 = 5$ $w_2 = 5$ $w_3 = 4$  $w_4 = 7$ $w_5 = 6$ $w_0 = 15$
SNR=9dB	$w_1 = 5$ $w_2 = 4$ $w_3 = 4$  $w_4 = 9$ $w_5 = 6$ $w_0 = 15$	$w_1 = 3$ $w_2 = 8$ $w_3 = 3$  $w_4 = 3$ $w_5 = 3$ $w_0 = 11$	$w_1 = 1$ $w_2 = 5$ $w_3 = 1$  $w_4 = 1$ $w_5 = 3$ $w_0 = 6$
SNR=15dB	$w_1 = 8$ $w_2 = 3$ $w_3 = 3$  $w_4 = 6$ $w_5 = 5$ $w_0 = 9$	$w_1 = 2$ $w_2 = 3$ $w_3 = 1$  $w_4 = 7$ $w_5 = 3$ $w_0 = 8$	$w_1 = 7$ $w_2 = 2$ $w_3 = 3$  $w_4 = 3$ $w_5 = 2$ $w_0 = 10$

Fig. 4. Optimal  $\mathcal{L}$ -M-S 5 filters for images Lena, airfield, and bridge for different SNR values. In all cases the optimal stack filters turned out to be WOS filters with weights  $w_1, \dots, w_5$  and threshold  $w_0$ , with the corresponding structures selected for the median filters.

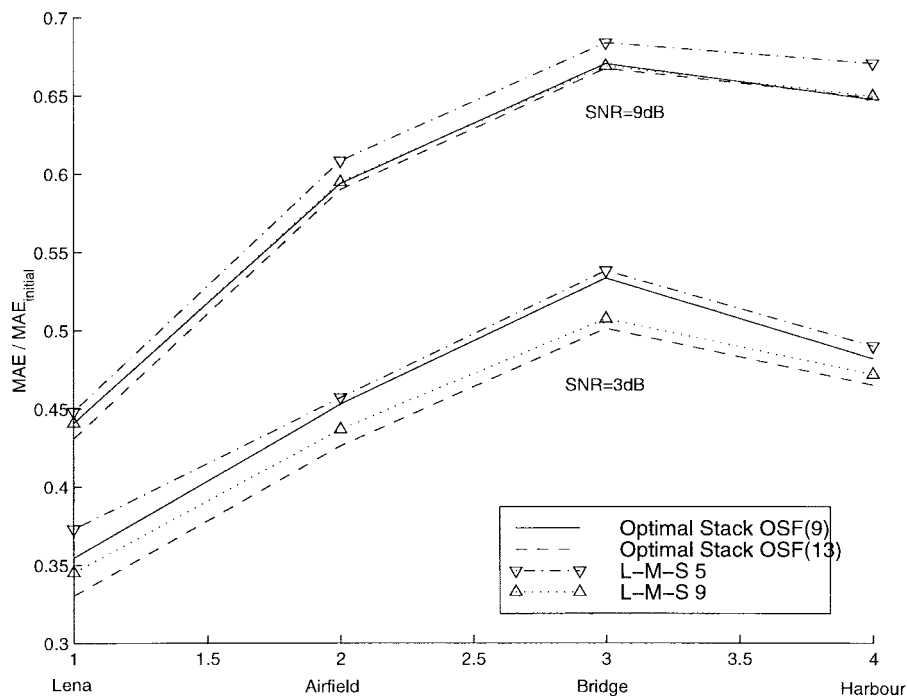


Fig. 5. MAE obtained over the test sets (three-quarters of the images) for images Lena, airfield, bridge, and harbor, corrupted at 3 and 9 dB, when filtered with optimally designed  $\mathcal{L}$ -M-S and stack filters (designed using the top-left quarter of the corresponding image).

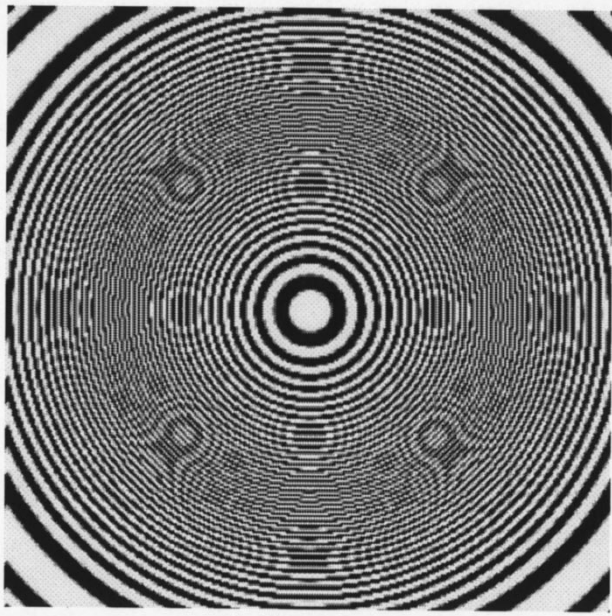


Fig. 6. Test image.

A simple example is used to illustrate the definition. The overall processing mask  $\mathbf{X} = [X_1 \ X_2 \ X_3 \ X_4]$  contains  $P = 4$  pixels

$$\begin{array}{ccc} & X_1 & \\ X_2 & X_3 & X_4 \end{array}$$

where  $X_3$  corresponds to the current pixel. We may define the library of processing subwindows by the set of four subwindows  $\mathcal{L} = \{\mathcal{L}_1, \mathcal{L}_2, \mathcal{L}_3, \mathcal{L}_4\}$  where  $\mathcal{L}_1 = \{X_1 \ X_2 \ X_3\}$ ;  $\mathcal{L}_2 = \{X_2 \ X_3 \ X_4\}$ ;  $\mathcal{L}_3 = \{X_1 \ X_2 \ X_4\}$ ;  $\mathcal{L}_4 = \{X_1 \ X_3 \ X_4\}$ . In the class  $\{\mathcal{L}, N = 2\}$  there will be  $C_4^2 = 6$  different possible selections of indices  $\ell_1$  and  $\ell_2$ . One example of  $\mathcal{L}$ -M-S filter can be obtained by taking  $\ell_1 = 1, \ell_2 = 3$  (which leads to  $\mathbf{U}_1 = \mathcal{L}_1, \mathbf{U}_2 = \mathcal{L}_3$ ) and the stack filter  $SF_{\mathbf{f}}([V_1, V_2]) = \min(V_1, V_2)$  (for which  $\mathbf{f} = [0 \ 0 \ 0 \ 1]^T$ ), resulting in the overall filter output  $Y = \min(\text{median}(X_1, X_2, X_3), \text{median}(X_1, X_2, X_4))$ .

Several possibilities exist for the implementation of the  $\mathcal{L}$ -M-S filters: the first is to apply the two-stage filtering as described above, and exemplified in Fig. 1. The second possible implementation comes from observing that any  $\mathcal{L}$ -M-S filter can be represented as a stack filter. This property follows immediately from (1), noting the fact that a composition of stack filters is a stack filter [7]. Now we can apply all implementation techniques available for stack filters to implement any  $\mathcal{L}$ -M-S filter. Furthermore,  $\mathcal{L}$ -M-S filters inherit all properties of stack filters, e.g. since we may easily define a dual of a stack filter, (which is also a stack filter) we may define similarly the dual of a  $\mathcal{L}$ -M-S filter. We note here that  $\mathcal{L}$ -M-S filters are stable to duality operator: the dual of a  $\mathcal{L}$ -M-S filter is a  $\mathcal{L}$ -M-S filter having the same subwindows  $(\ell_1, \dots, \ell_N)$  for the median filtering level [3].

### III. OPTIMAL DESIGN OF $\mathcal{L}$ -M-S FILTERS

The proposed architecture offers many degrees of freedom, and finding an optimal solution in a  $\{\mathcal{L}, N\}$  filter class is not a trivial task. For a given library  $\mathcal{L}$  of  $K$  subwindows there are  $C_K^N$  possible selections of subwindows; and for every set of selected subwindows, there are  $\Psi(N)$  stack filters ( $\Psi(N)$  is much larger than  $2^{2^{N/2}}$  [2]).

If the median subwindows on the first filtering level are fixed, a fast optimal design procedure under the MAE criterion [5] for the

stack filter  $SF_{\mathbf{f}}$  can be used, and the solution is rapidly obtained for small values of  $N$  ( $N \leq 13$ ). The stack filter of the second level has a reduced design complexity versus the stack filter applied directly to the  $P$  elements of the overall processing mask  $\mathbf{X}$ , whenever  $N < P$  (which is the only case considered here). A training set is supposed to be given, consisting of a desired image and an input (corrupted) image.

In this work, a recursive design procedure for the filtering structure is proposed, combining the selection of different subwindows from the given library  $\mathcal{L}$  with the optimal stack filter design. First the MAE-optimal  $\mathcal{L}$ -M-S filter with  $N = 1$  is designed, observing that it will reduce to a median filter, since the stack filter with one input is the identity filter  $SF_{\mathbf{f}}(V_1) = V_1$ . The values  $\text{MAE}_i$  resulted after filtering the input image with the median with processing window  $\mathcal{L}_i$  are compared for  $i = 1, \dots, K$ , and the index  $i_{\min}$  for which the minimum of  $\text{MAE}_i$  is achieved is assigned to  $\ell_1^* = i_{\min}$ , resulting in the optimal  $\mathcal{L}$ -M-S filter with the structure  $\{\mathcal{L}, 1\}$ .

Now suppose we have available a suboptimal filter with the structure  $\{\mathcal{L}, k-1\}$  and we want to extend this filter to the structure  $\{\mathcal{L}, k\}$ , by leaving unchanged the  $k-1$  median filters and only adding a new median filter, with a subwindow to be determined, and redesigning the stack filter. The best extension can be checked by evaluating the MAE of all possible extended  $\mathcal{L}$ -M-S filters, when including a new median filter having a subwindow from the library which has not yet been used and designing the new optimal filter for this situation. By repeating this process from  $k = 2$  to  $N$  a suboptimal  $\mathcal{L}$ -M-S with the structure  $\{\mathcal{L}, N\}$  will be obtained.

To derive the stack filter, the optimal procedure presented in [5] is used. In the first stage of the optimal design of a stack filter for  $N$  input variables, a  $2^N$ -length vector of *cost coefficients*, denoted  $\mathbf{C}$  is computed from the training data set (desired image and a noise corrupted image) [5]. The computation of the cost coefficients requires scanning the whole data set, which is the most expensive part of the design. We will avoid the repetition of this stage in our successive applications of optimal stack filter design necessary for  $\mathcal{L}$ -M-S filter design, and a single scanning of the data set will be required.

The cost coefficients  $\mathbf{C}$  for the overall processing window  $\mathbf{X}$  are first computed. Then, each time a stack filter is designed, the necessary cost coefficients,  $C^{[1]}$ , are computed from  $\mathbf{C}$ , using the structure information provided by the selected subwindows from  $\mathcal{L}$  and the median filter Boolean function  $f^{\text{med}}$ , as explained below. Since  $\mathbf{U}_i = \mathcal{L}_{\ell_i} \subset \mathbf{X}$  we may immediately find  $\mathbf{u}_i$  from  $\mathbf{x}$ , where the binary vectors  $\mathbf{x}$  and  $\mathbf{u}_i$  are obtained by respectively thresholding the values in the processing windows  $\mathbf{X}$  and  $\mathbf{U}_i$ , and therefore we will write  $\mathbf{u}_i(\mathbf{x})$ . When analyzing in the threshold domain the effect of the median filters of the first layer of the  $\mathcal{L}$ -M-S filter, we observe that the binary window  $\mathbf{x}$  is transformed into the binary window

$$\mathbf{v}(\mathbf{x}) = [f^{\text{med}}(\mathbf{u}_1(\mathbf{x})), \dots, f^{\text{med}}(\mathbf{u}_k(\mathbf{x}))]. \quad (2)$$

Therefore, the cost associated with the binary window  $\mathbf{v}$ , obtained by thresholding the entries in the input of stack filter  $\mathbf{V}$ , will be

$$C^{[1]}(\mathbf{v}) = \sum_{\mathbf{x} | \mathbf{v}(\mathbf{x}) = \mathbf{v}} C(\mathbf{x}) \quad (3)$$

and finally the stack filter will be designed such that to minimize

$$\text{MAE}(\mathbf{f}) = C_0 + \sum_{\mathbf{v}} C^{[1]}(\mathbf{v})f(\mathbf{v}) \quad (4)$$

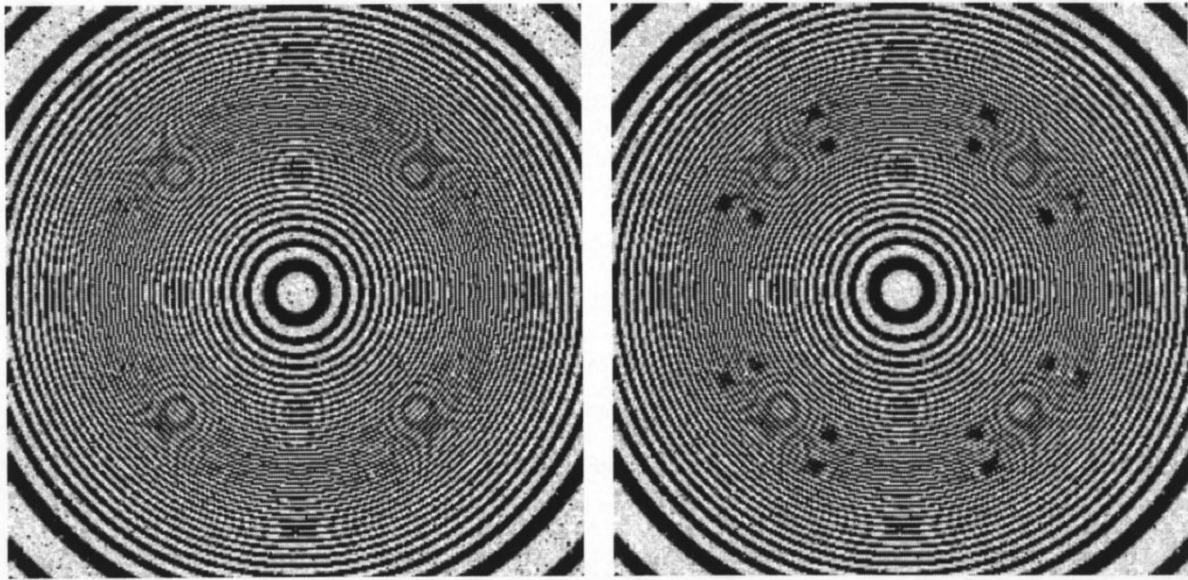


Fig. 7. Result of filtering with  $\mathcal{L}$ -M-S 9 filter (left) and with unidirectional multistage median filter (right). The input image is corrupted at SNR = 9 dB.



(a)



(b)



(c)



(d)

Fig. 8. Original and corrupted images and image filtered with  $\mathcal{L}$ -M-S filter. (a) Original harbor image. (b) Filtered with  $\mathcal{L}$ -M-S 9 filter. (c) Detail from original. (d) Corrupted original at SNR = 3 dB.

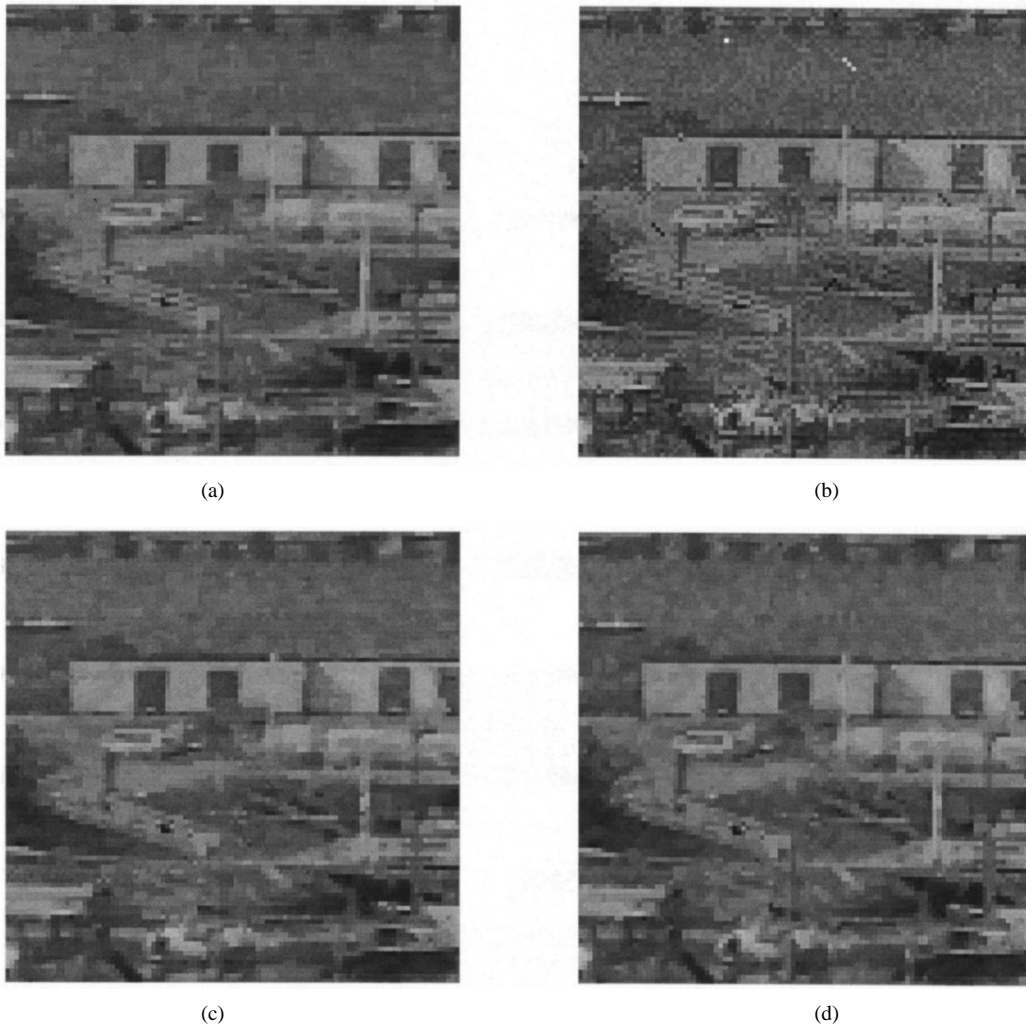


Fig. 9. Images filtered with (a)  $\mathcal{L}$ -M-S 9 filter; (b) UMM filter; (c)  $\mathcal{L}$ -M-S 5 filter; (d) optimal stack-9 filter.

where  $C_0$  is a constant denoting the mean value in the desired image [5]. We can summarize now the  $\mathcal{L}$ -M-S filter design procedure: the indices of the subwindows to be used by the median filters are selected recursively. At stage  $k$  we test the performance of extensions of the previous stage filter  $\{\mathcal{L}, k-1\}$ , and select the extension which improves performance the most. The evaluation of the extension  $\ell_1^*, \ell_2^*, \dots, \ell_{k-1}^*, \ell_k$  is obtained by finding first the correspondence (2), between the vectors  $\mathbf{v} \in \{0,1\}^k$  and  $\mathbf{x} \in \{0,1\}^P$ , then computing the cost coefficients (3) and finally applying the optimal stack filter design [5] and finding the MAE (4) corresponding to the optimal filter.

#### IV. EXPERIMENTAL RESULTS

To analyze the performance of the proposed filtering architecture, under the above outlined design procedure, a noise rejection application is considered. A processing mask  $\mathbf{X}$  of 13 pixels is defined in Fig. 2 (the central pixel being the current one). A library of  $K = 57$  subwindows for the median filtering level is proposed, the elements of the library being selected to cover most of the possible small connected details in an image. The following subwindows have been selected: three-pixel connected subwindows contained in a  $3 \times 3$  neighborhood of the central pixel; three-pixel horizontal and vertical connected subwindows starting at the central pixel and extending beyond its  $3 \times 3$  square neighborhood; five-pixel vertical

and horizontal subwindows; five-pixel cross subwindows; the central pixel itself. The elements of the library are presented in Fig. 3.

In the experiments,  $512 \times 512$  images (Lena, airfield, harbor, and bridge) are used. These images are corrupted by additive noise having a Gaussian contaminated distribution. The contamination is chosen to obtain impulsive noise (long-tailed distribution), at different signal-to-noise (SNR) values. Two different values for the number of median filters on the first level are considered:  $N = 5$ , for the filter denoted by  $\mathcal{L}$ -M-S 5 and  $N = 9$  for the filter denoted by  $\mathcal{L}$ -M-S 9. The filtering results are compared with the performance of the optimal stack filter (OSF) for the  $3 \times 3$  square and 13-pixel window  $\mathbf{X}$ . The optimal design was performed using as training set the top-left quarter of the desired image and the corresponding corrupted image. The reported performance was evaluated over the remaining three quarters of each image. The results are presented in Fig. 5, while several images and details are shown in Figs. 8 and 9.

In all experiments the performance of  $\mathcal{L}$ -M-S filters is close to that of some corresponding optimal stack filter. The  $\mathcal{L}$ -M-S 5 filter performs similarly to the optimal stack on  $3 \times 3$  square processing mask (OSF9), and the  $\mathcal{L}$ -M-S 9 filter performs as well as the optimal stack on the overall processing mask, OSF13 and outperforms OSF9. In Fig. 4, the subwindows selected for the median filtering level in  $\mathcal{L}$ -M-S 5 for images Lena, airfield, and bridge at four different SNR's are illustrated (the training set contained now all four quarters of the images).

Figs. 6 and 7 demonstrate the improved detail preservation performance of  $\mathcal{L}$ -M-S 9 filter, compared to that of unidirectional multistage median (UMM) filter [1].

## V. CONCLUSIONS

In this correspondence, a new class of filters, extending the class of multistage median filters [1], is proposed. The properties and filtering performance of  $\mathcal{L}$ -M-S filters are presented for an image noise rejection application. The design examples for various images and corruption scenarios reveal a performance close to that of optimal stack filters at a lower design cost, when a particular library  $\mathcal{L}$  of subwindows for the median filters, based on connectivity criteria, is used.

## REFERENCES

- [1] G. R. Arce and R. E. Foster, "Detail preserving ranked-order based filters for image processing," *IEEE Trans. Acoust., Speech, Signal Processing*, vol. 37, pp. 83–98, Jan. 1989.
- [2] E. J. Coyle and J.-H. Lin, "Stack filters and the mean absolute error criterion," *IEEE Trans. Acoust., Speech, Signal Processing*, vol. 36, pp. 1244–1254, Aug. 1988.
- [3] D. Petrescu, "Optimal design and image processing applications of Boolean, stack and morphological filtering," Ph.D. dissertation, Tampere Univ. Technol., Tampere, Finland, 1997.
- [4] A. Nieminen, P. Heinonen, and Y. Neuvo, "A new class of detail-preserving filters for image processing," *IEEE Trans. Pattern Anal. Machine Intell.*, vol. PAMI-9, pp. 74–91, Jan. 1987.
- [5] I. Täbuş, D. Petrescu, and M. Gabbouj, "A training framework for stack and Boolean filtering—Fast optimal design procedures and robustness case study," *IEEE Trans. Image Processing, Spec. Issue Nonlinear Image Processing*, vol. 5, pp. 809–826, June 1996.
- [6] X. Wang, "Generalized multistage median filter," *IEEE Trans. Image Processing*, vol. 1, pp. 543–545, Oct. 1992.
- [7] P. D. Wendt, E. J. Coyle, and N. C. Gallagher, Jr., "Stack filters," *IEEE Trans. Acoust., Speech, Signal Processing*, vol. 34, pp. 898–911, Aug. 1986.
- [8] R. Yang, Y. Lin, M. Gabbouj, J. Astola, and Y. Neuvo, "Optimal weighted median filtering under structural constraints," *IEEE Trans. Signal Processing*, vol. 43, pp. 591–604, Mar. 1995.
- [9] X. Yang and P. S. Toh, "Adaptive fuzzy multilevel median filter," *IEEE Trans. Image Processing*, vol. 4, pp. 680–682, May 1995.

## Optimal Bit Allocation and Best-Basis Selection for Wavelet Packets and TSVQ

Jill R. Goldschneider and Eve A. Riskin

**Abstract**— To use wavelet packets for lossy data compression, the following issues must be addressed: quantization of the wavelet subbands, allocation of bits to each subband, and best-basis selection. We present an algorithm for wavelet packets that systematically identifies all bit allocations/best-basis selections on the lower convex hull of the rate-distortion curve. We demonstrate the algorithm on tree-structured vector quantizers used to code image subbands from the wavelet packet decomposition.

**Index Terms**— Best basis selection, bit allocation, compression, tree-structured vector quantization, wavelet packets.

## I. INTRODUCTION

Lossy transform data compression, especially of image data, is typically more successful when local frequency characteristics, such as abrupt changes due to edges, are preserved. Traditional Fourier analysis decomposes a signal into a sum of orthogonal trigonometric functions, creating a frequency representation in which the temporal or spatial information of the data is distributed across all frequencies. In a Fourier representation, the energy of discontinuities is spread across a broad range of frequencies, and location information is represented in the phase of the frequency coefficients. Hence, discontinuities cannot be compactly represented in the Fourier domain. This loss of compactness in localizing discontinuities can be detrimental when handling images, which typically contain a large number of discontinuities. Instead, a time-frequency or space-frequency representation of a signal can be used to capture local frequency behavior of signals and images.

Wavelets [1], [2] are an important tool for space-frequency analysis in which simple, orthonormal bases of  $L^2(R^d)$  are built with good localization properties in both space and frequency, providing a powerful framework for image coding. Orthonormal wavelet packets are created by decomposing a signal into smooth (**S**) and detail (**D**) subbands corresponding to different orthogonal, critically sampled frequency bands. Each subband is then further decomposed into smooth and detail subbands. By selecting the wavelet packet subbands that are better adapted to the frequency characteristics of the signal, one may achieve better (e.g., lower entropy, rate, or distortion) signal representation.

To use wavelet packets for data compression, the following issues must be addressed: the quantization of the wavelet subbands, the allocation of bits to each subband, and the selection of subbands (i.e., best-basis selection). An algorithm for joint bit allocation/best-

Manuscript received February 12, 1998; revised December 22, 1998. This work was supported by a NASA Graduate Student Fellowship in Global Change Research, an NSF Young Investigator Award, U.S. Army Research Grant DAAH004-96-1-0255, and a Sloan Research Fellowship. This work appeared in part in the Proceedings of the 1998 International Conference on Acoustics, Speech, and Signal Processing. The associate editor coordinating the review of this manuscript and approving it for publication was Prof. Kannan Ramchandran.

J. R. Goldschneider is with MathSoft, Inc., Seattle, WA 98109-3044 USA (e-mail: jrgold@statsci.com).

E. A. Riskin is with the Department of Electrical Engineering, University of Washington, Seattle, WA 98195-2500 USA (e-mail: riskin@ee.washington.edu).

Publisher Item Identifier S 1057-7149(99)06829-3.